

Article

## Comprehensive Design and Propagation Study of a Compact Dual Band Antenna for Healthcare Applications

Mohammad Monirujjaman Khan <sup>1,2,\*</sup>, Qammer H. Abbasi <sup>1,3,†</sup> and Ratil Hasnat Ashique <sup>2,†</sup>

<sup>1</sup> School of Electronic Engineering and Computer Science, Queen Mary University of London, Mile End Road, London E1 4NS, UK; E-Mail: monirkhan.qmul@gmail.com

<sup>2</sup> Department of Electrical and Electronic Engineering, Primeasia University, Kemal Ataturk Avenue, Banani, Dhaka-1213, Bangladesh; E-Mail: ratil.eee05@gmail.com

<sup>3</sup> Department of Electrical and Computer Engineering, Texas A&M University at Qatar, PO Box 23874, Education City Doha, Qatar; E-Mail: majorqam@hotmail.com

† These authors contributed equally to this work.

\* Author to whom correspondence should be addressed; E-Mail: monirkhan.qmul@gmail.com or monirujjaman.khan@primeasia.edu.bd; Tel.: +88-01-779-006-296 or +88-02-982-2133 (ext. 167); Fax: +88-02-982-0868.

Academic Editor: Stefan Fischer

Received: 11 December 2014 / Accepted: 11 March 2015 / Published: 2 April 2015

---

**Abstract:** In this paper, a dual band planar inverted F antenna (PIFA) has been investigated for cooperative on- and off-body communications. Free space and on-body performance parameters like return loss, bandwidth, radiation pattern and efficiency of this antenna are shown and investigated. The on- and off-body radio propagation channel performance at 2.45 GHz and 1.9 GHz have been investigated, respectively. Experimental investigations are performed both in the anechoic chamber and in an indoor environment. The path loss exponent has been extracted for both on- and off-body radio propagation scenarios. For on-body propagation, the path loss exponent is 2.48 and 2.22 in the anechoic chamber and indoor environment, respectively. The path loss exponent is 1.27 for off-body radio propagation situation. For on-body case, the path loss has been characterized for ten different locations on the body at 2.45 GHz, whereas for off-body case radio channel studies are performed for five different locations at 1.9 GHz. The proposed antenna shows a good on- and off-body radio channel performance.

**Keywords:** dual band; planar inverted F antenna; on/off-body communications; on/off-body radio channel; path loss; body area networks; body-centric wireless communications

---

## 1. Introduction

Wireless sensor and body area networks are attractive solutions that can be used in healthcare applications, which will enable constant monitoring of health data and constant access to the patient. It was estimated that wireless sensor solutions could save \$25 billion worldwide in annual healthcare costs by reducing hospitalizations and extending independent living for the elderly [1]. Body-centric wireless communications (BCWCs) is a central point in the development of fourth generation mobile communications. In body-centric wireless communication, the wireless connectivity between body-centric units is provided through the deployment of sensor and compact antennas [2]. Body-worn antennas can suffer from reduced efficiency and gain due to electromagnetic absorption in tissue, radiation pattern fragmentation, variations in feed point impedance and frequency detuning [3,4].

In common healthcare monitoring scenarios, it is very important for the antenna to communicate among the devices mounted on the body as well as off-body devices. There are two main channels of interest for wireless body area networks: off-body and on-body. The on-body-communications-describe the link between body mounted devices communicating wirelessly, while off-body communication defines the radio link between body worn devices and base units or mobile devices located in surrounding environment [2].

Recently, there has been increasing interest in research and development for designing wearable antennas. In previous studies, most researchers have designed the antennas for on-body communications at 2.45 GHz and ultra wideband (UWB) at 3.1~10.6 GHz [3–27]. Researchers also investigated the on-body radio propagation channel both in narrowband at 2.45 GHz and ultra wideband (3~10 GHz) technologies [3–27]. However, there is a need of antenna design for cooperative on-body and off-body communications. In this paper, a dual band planar inverted F antenna (PIFA) is designed and the performance parameters of that antenna are investigated in close proximity to the human body. The proposed PIFA operates at two different frequency bands, 2.45 GHz (ISM band) and 1.9 GHz (PCS band). The 2.45 GHz is used for the communication (on-body) among the devices located over the human body surface and 1.9 GHz is used for the communication from body mounted devices to off-body units (off-body). The on-body radio channel behavior at 2.45 GHz and off-body radio channel performance at 1.9 GHz of the proposed PIFA has also been experimentally investigated.

The rest of the paper is organized as follows; Section 2 discusses about the PIFA antenna design and its free space and on-body performance parameters, Section 3 talks about on-body radio channel measurements setting and on-body results, section 4 presents off-body radio channels measurement settings and results, and finally Section 5 draws the conclusion of the presented study.

## 2. On-Body Performance Parameters of Dual Band PIFA

### 2.1. Antenna Design

The schematic diagram and fabricated dual band Planar Inverted F Antenna (PIFA) are shown in Figure 1. The antenna was modeled on FR4 substrate with a thickness of 1.57 mm and a relative permittivity of 4.6. At the backside of this antenna there is a full ground plane. The total height of the antenna is 6.92 mm and the overall ground plane size is  $63 \times 34 \text{ mm}^2$ . The dimension of PIFA elements are given in Table 1 and shown in Figure 1c.

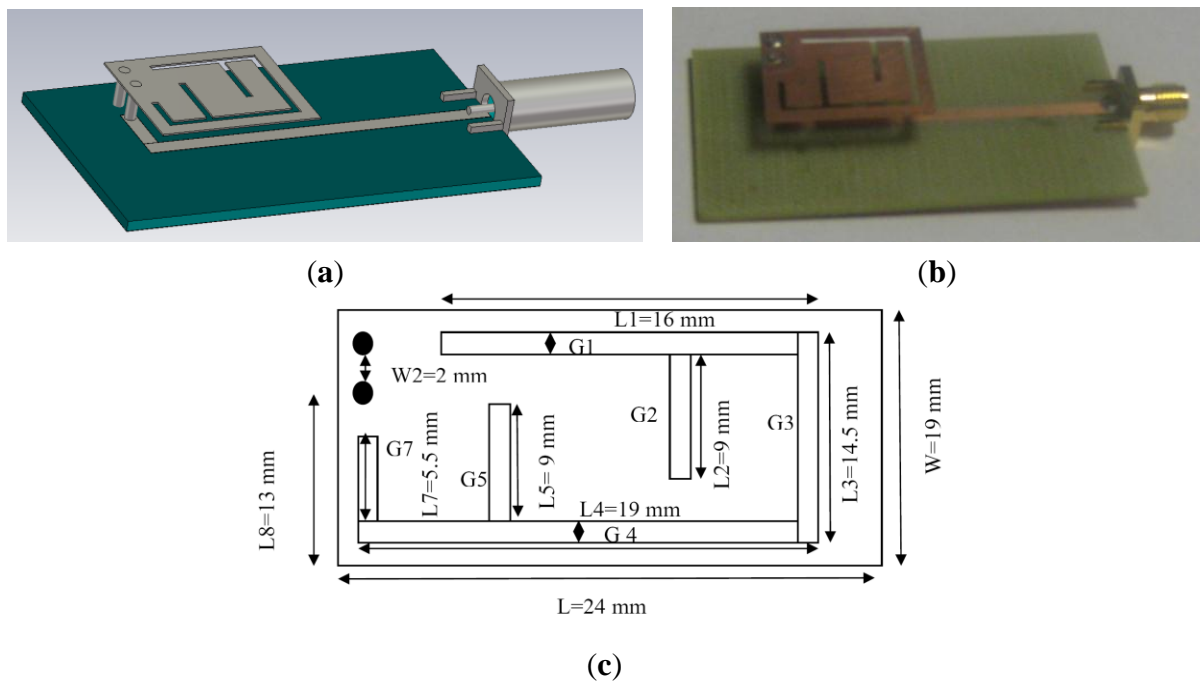


**Figure 1.** (a) Software design; (b) Fabricated version; (c) Schematic diagram of the dual band planar inverted F antenna PIFA.

**Table 1.** Dimension parameters of the dual band planar inverted F antenna (PIFA).

Antenna Elements	Dimension
Ground plane	$63 \times 34 \text{ mm}^2$
Slit width (G)	1 mm
Shoring pin height	6.92 mm
Shoring pin diameter	1.6 mm
Feeding pin height	5.3 mm
Feeding pin diameter	1.6 mm
Width of feed line	2.4 mm
Length of feed line	51 mm
Length of Radiating PIFA (L)	24 mm
Width of Radiating PIFA (W)	19 mm
Thickness of Radiating PIFA	0.25 mm
Total length of the slit (L1~L7)	72 mm
Antenna volume	$63 \times 34 \times 7 \text{ mm}^3$

The dual band PIFA is excited using a microstrip feed, which is connected to the feeding pin. The gap between the shorting pin and the feeding pin is 2 mm. The gap between the shorting pin and feeding pin has an effect on the impedance matching of the antenna. The function of the shorting pin of the PIFA is to minimize the size of the antenna and to achieve the impedance matching [28]. The antenna is proposed to use in body-centric wireless communications where communication is necessary both to the devices on the body and to the external off body network nodes. The radiating rectangular PIFA works at the lower frequency band (1.9 GHz) for communication from body mounted devices to off-body devices. The double F shape slits are introduced on the antenna structure with a view to achieve dual band characteristics, *i.e.*, the higher frequency band (2.45 GHz) for the communication over the body surface to communicate with other body worn devices.

The bandwidth of the dual band PIFA can be achieved by varying radiating element size, changing the width of the shorting pin, and adding slot on the ground plane. The antenna radiation and impedance bandwidth are dependent on the height of the radiator to the ground. The bigger the air gap between radiator and ground plane, the greater the bandwidth and gain of the proposed dual band PIFA. The physical size of the proposed PIFA is compact.

## 2.2. Return Loss

The antenna was first simulated in free space and then it was simulated placing on the human phantom (right side of the chest) in order to study the effect of human body on the antenna performance parameters. Computer Simulation Technology microwave studio™ software was used for antenna design and simulation purposes. The human body applied is the commonly available detailed multi-layer model (2) namely the visible male model developed by the US air force [29]. The resolution of the model applied is 4 mm with human tissues electrical properties defined at 2.45 GHz and 1.9 GHz, respectively, for all organs and tissues used including heart, lungs, muscle, fat, skin, *etc.* [30, 31]. During the simulation, the antenna was placed at 1 mm away from the human body. Figure 2 shows the location and orientation of the dual band planar inverted F antenna (PIFA) on the human body.

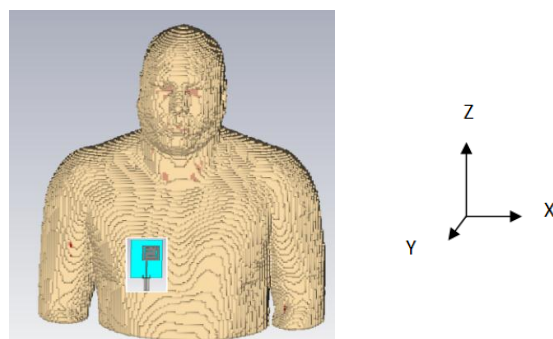


**Figure 2.** Location and orientation of the dual band PIFA on the human body.

The free space and on-body return loss responses of the proposed dual band PIFA are shown in Figure 3. Dual band characteristic of the antenna is achieved with a minimum return loss of  $-25.60$  dB at 1.914 GHz for the lower frequency band and  $-30.38$  dB at 2.462 GHz for the higher frequency band when the antenna is simulated in free space. When the antenna is simulated being placed on the human body, 0.5 MHz or 0.02% frequency detuning is noticed at the higher frequency band, while 5 MHz or 0.26%

frequency detuning is noticed at the lower frequency band. It is noticed from the simulation results that this antenna does not experience significant frequency detuning from the free space resonance at both frequency bands when placed on the body due to shielding provided by the full ground plane at the backside of the antenna.

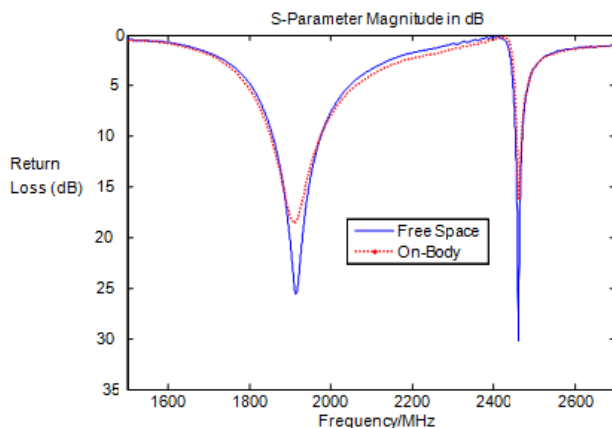


**Figure 3.** Simulated free space and on-body (1 mm away from human body) return loss responses of the dual band PIFA.

The return loss response of the dual band PIFA was also measured first in free space and then on a real human test subject. During the measurement, the antenna was placed on different distances from the body (right side of the chest) as directed on the body, 1 mm, 4 mm, 8 mm and 16 mm away from the human body. The measurement was performed in the anechoic chamber in the Antenna Measurement Laboratory at Queen Mary University of London. Figure 4 shows measured return loss curves of the dual band PIFA when it is placed on the right side of the chest varying the distance between the antenna and the body. Results illustrate that when the antenna is placed on the human body, a maximum up to 40 MHz (2.13 %) frequency detuning from the free resonance frequency is noticed at the lower frequency band while at higher band there is no frequency detuning. At lower frequency band, the frequency detuning decreases as the distance between the body and the antenna increases.

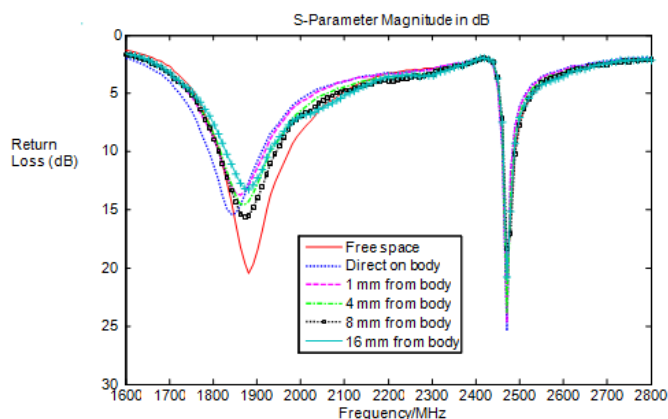


**Figure 4.** Measured free space and on-body return loss responses of the dual band PIFA.

The bandwidth and other performance parameters of this antenna have also been investigated. Free space and on-body performance parameters of the antenna are tabulated in the Table 2. In free space

simulation, at 10 dB impedance bandwidth, the lower band achieves 117.47 MHz of bandwidth (6.14%) while the higher band shows 17 MHz (0.68%). It is noticed that the simulated bandwidth of the antenna increases to 5.18 MHz at lower frequency band and decreases to 4.47 MHz for the higher band when it is placed on the human body. The proposed dual band PIFA shows very good on-body gain at both frequency bands. When the antenna is placed on the human body, it experiences an increase of 0.02 dB gain at lower frequency band, whereas a decrease of 0.61 dB gain is noticed for the higher frequency band. The proposed dual band PIFA demonstrates very good on-body radiation efficiency of 58.03% and 52.0% for 1.9 GHz and 2.45 GHz, respectively, when it is placed 1 mm away from the body. The antenna shows very good performance in close proximity to the human body.

**Table 2.** Simulated free space and on-body performance parameters of the PIFA.

Parameter	Low Band		High Band	
	Free Space	On-body	Free Space	On-body
Resonance $f_c$ (MHz)	1914	1909	2462.5	2463
Bandwidth (10 dB)	117.47	122.65	17	12.53
Gain (dBi)	3.72	3.74	3.69	3.08
Radiation efficiency (%)	98.98	58.03	99.30	52.0

**2.3. Radiation Pattern**

The radiation pattern of the antenna is extracted from simulation results. The radiation pattern has been first simulated in free space and then on the real human body. Figure 5 shows the antenna location and orientation for on-body radiation pattern measurement. The free space and on-body simulated radiation patterns at 2.45 GHz of the dual band PIFA is shown in Figure 6. Figure 7 show the free space and on-body radiation patterns of the PIFA at 1.9 GHz. When the dual band PIFA is placed on the body (1 mm away from the body), at 2.45 GHz, the radiation pattern in the XZ plane does not deform, but the power level reduces in one direction while in the YZ plane slight deformation of the radiation pattern is noticed, which is due to the presence of the human body. At 1.9 GHz, the radiation patterns in both XY and YZ planes deform very slight. In the YZ plane the antenna produces directive radiation patterns in both planes, which are good for communication from on-body to off-body units. The antenna shows very good on-body radiation performance.

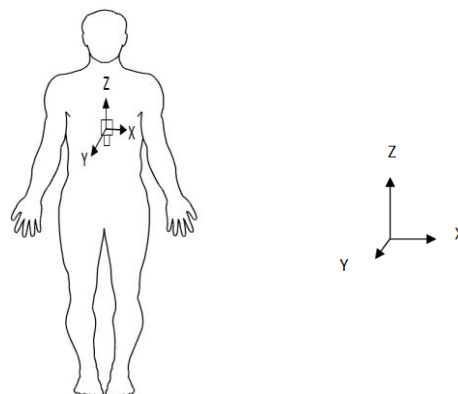


**Figure 5.** The antenna location and orientation for on-body radiation pattern.

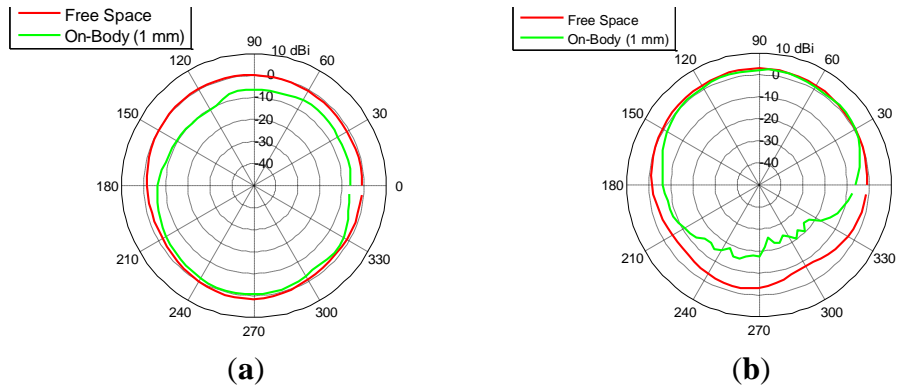


**Figure 6.** Free space and on-body radiation patterns of the dual band PIFA at 2.45 GHz; (a) XZ plane at 2.45 GHz and (b) YZ plane at 2.45 GHz.

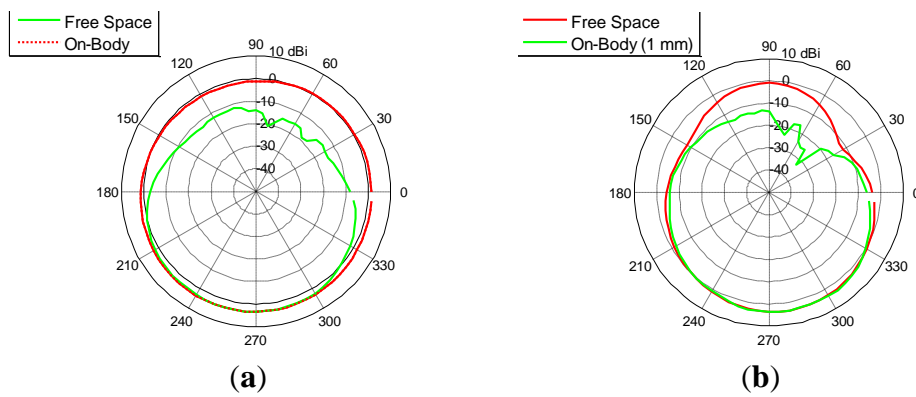


**Figure 7.** Free space and on-body radiation patterns of the dual band PIFA antenna at 1.9 GHz (a) XY plane at 1.9 GHz and (b) YZ plane at 1.9 GHz.

### 3. Investigation of On-Body Radio Propagation Channels at 2.45 GHz

In this study, the on-body radio channel performance at 2.45 GHz of the dual band PIFA has been experimentally investigated. The  $S_{21}$  measurements of the proposed PIFA at 2.45 GHz were performed in an anechoic chamber and in the indoor environment. An average-sized real male test subject, with a height of 1.74 m and a weight of 80 kg was used. A HP8720ES vector network analyzer (VNA) was used to measure the transmission response ( $S_{21}$ ) between two PIFAs placed on the body. The transmitter antenna connecting with the cable was placed on the left waist, while the receiver antenna connecting with the cable was successively placed on 31 different locations on the front part of the standing human body; as shown in Figure 8. The test subject was standing still during the measurements and, for each receiver location and measurement scenario, 10 sweeps were considered. The effects of the cable were calibrated out before the measurement. The path loss for the different receiver locations was calculated directly from the measurement data of  $S_{21}$  (10 sweeps) averaging at 2.45 GHz.

The on-body measurement campaigns were first performed in the anechoic chamber and then repeated in the Body-Centric Wireless Sensor Laboratory at Queen Mary, University of London [32]. The total area of the lab is 45 m<sup>2</sup>, which includes a meeting area, treadmill machine, workstations and a hospital bed for healthcare applications.

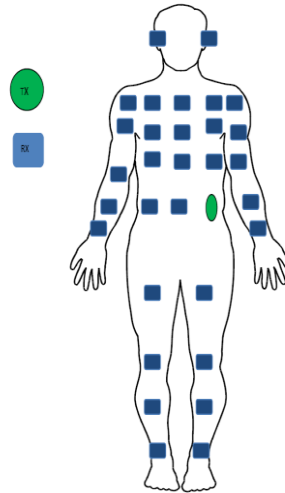


**Figure 8.** The transmitter antenna is on left waist and the receiver antenna is attached to 31 different locations on the body for on-body radio propagation measurement at 2.45 GHz.

### 3.1. Path Loss vs. Distance

The path loss was modeled as a function of distance for 31 different receiver locations for propagation along the front part of the body. The average received signal decreases logarithmically with distance for both indoor and outdoor environments as explained in [33].

$$PL_{dB}(d) = PL_{dB}(d_0) + 10\gamma \log\left(\frac{d}{d_0}\right) + X_\sigma \tag{1}$$

where  $d$  is the distance between transmitter and receiver,  $d_0$  is a reference distance set in measurement (in this study it is set to 10 cm),  $PL_{dB}(d_0)$  is the path loss value at the reference distance, and  $X_\sigma$  is the shadowing fading. The parameter  $\gamma$  is the path loss exponent that indicates the rate at which the path loss increases with distance [34].

A least-square fit technique was performed on the measured path loss for the 31 different receiver locations, (Figure 8) to extract the path loss exponent. Figure 9 shows the measured value and modeled path loss for on-body channels *versus* logarithmic transmitter (Tx)-receiver (Rx) separation distance. In this study, the path loss exponent in the chamber is 2.67 and in the indoor it is 2.43 (Table 3). In the indoor environment, the path loss exponent was found to be lower compared to in the chamber. When measurements are performed indoors, the reflections from surroundings scatters increase the received power, causing reduction in the path loss exponent. A reduction of 8.99% was noticed in the indoor environment compared to the chamber. This antenna shows very good path loss exponent values both in the indoor environment and chamber for the propagation over the body surface. In [13], the path loss exponent was extracted at 2.45 GHz using printed monopole antenna for propagation over the human body. The same measurement setting and same test subject were used for that measurement case as was used for the PIFA case. For printed monopole antenna cases, the path loss exponent at 2.45 GHz was 3.71, whereas for the PIFA antenna cases, it was 2.43. Compared to the printed monopole antenna, PIFA shows very less path loss exponent value, which indicates that the PIFA has less link loss for on-body communication.



**Table 3.** On-body path loss parameters at 2.45 GHz.

Path Loss Parameters	Chamber	Indoor
$\gamma$	2.67	2.43
$PL_{dB}(d_0)$ (dB)	35	36.7
$\sigma$ (dB)	6.60	5.90

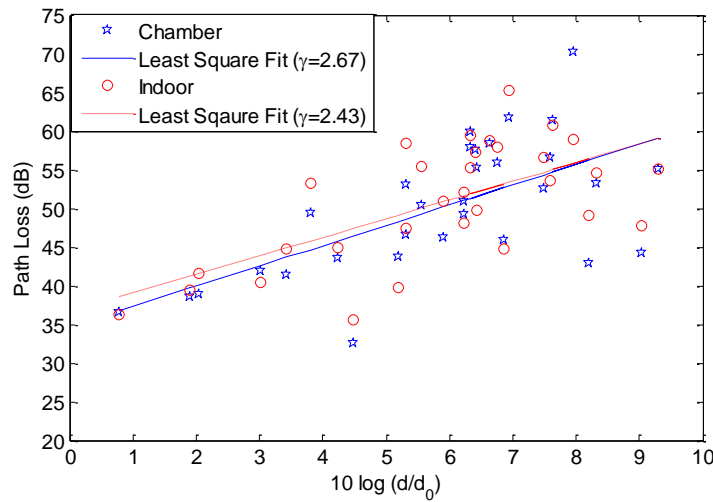


**Figure 9.** Measured and modeled path loss for on-body channel vs. logarithmic transmitter (Tx) and receiver (Rx) separation distance for the dual band PIFA at 2.45 GHz.

$X_\sigma$  is a zero mean, normal distributed statistical variable, and is introduced to consider the deviation of the measurements from the calculated average path loss. Figure 10 shows the deviation of measurements from the average path loss fitted to a normal distribution for both measurement cases. In this case, the standard deviation of the normal distribution is found to be slight lower in the indoor environment (Table 3).

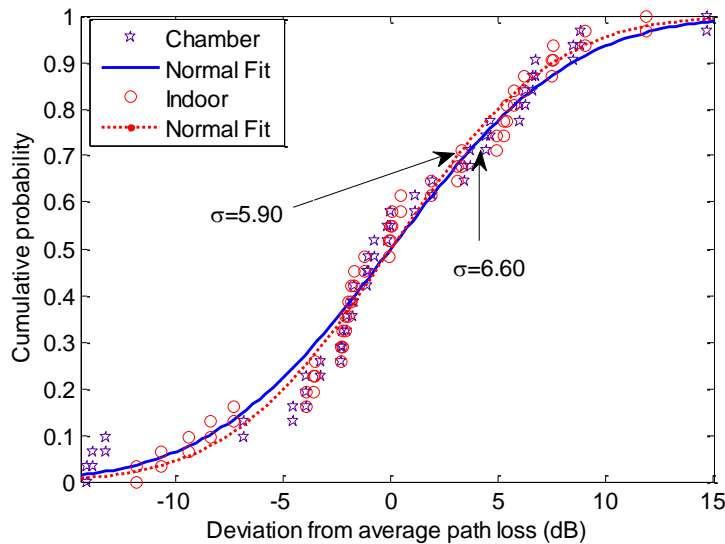


**Figure 10.** Deviation of measurement from the average path loss (fitted to normal distribution) for the dual band PIFA at 2.45 GHz.

*3.2. On-Body Radio Channel Path Loss Characterization at 2.45 GHz*

In this study, the path loss for ten different on-body radio channels at 2.45 GHz has been characterized and investigated (see Figure 11). In this case, the same measurement set up was applied as was applied for the previous case. In this scenario, the transmitter antenna was placed on the left waist and the receiver antenna was attached to ten different locations on the body.

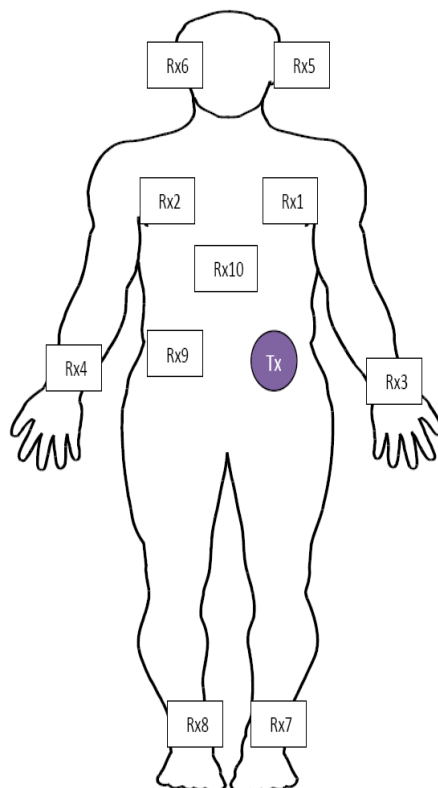


**Figure 11.** On-body radio propagation channel characterization measurement settings at 2.45 GHz showing the transmitter antenna is on the left waist while the receiver antenna is attached to 10 different locations on the body.

Figure 12 shows the comparison of path loss for left waist to ten different on-body links at 2.45 GHz measured in the chamber and in an indoor environment using dual band PIFA. It is noticed that both in the chamber and in indoor environment cases, the lowest path loss value is observed for the left waist to left chest and left wrist links while the highest is noticed for the right ear and right wrist channels. This is so happened because for left chest and left wrist channels, the communication distance between the transmitter antenna and the receiver antenna is less and there is direct Line-Of-Sight (LOS) communication but for the right ear and right wrist the communication distance between the receiver (Rx) antenna and transmitter (Tx) antenna is higher; moreover, the communication is blocked by human body and the presence of Non-Line-Of-Sight (NLOS) communication. The average path loss of ten different on-body channels is higher in the chamber than in the sensor lab as obvious due to the non-reflecting environment. The average of ten different on-body link’s path loss in the sensor lab is found to be 50.25 dB, while in the chamber it is found to be 51.04 dB. Right ear link experiences the highest difference in path loss. The path loss varies the most for the left waist to right ear link for two environment scenarios. According to the results

and analysis, it is noticed that this dual band PIFA shows very good on-body radio channel performance at 2.45 GHz. In [13], when measurement was performed using printed monopole antenna at 2.45 GHz the path loss for the left waist to left chest link was observed to be 54 dB but for the PIFA case for the same link, it is 40 dB. Results and analysis show that this PIFA will have less link loss for on-body communication channel at 2.45 GHz.

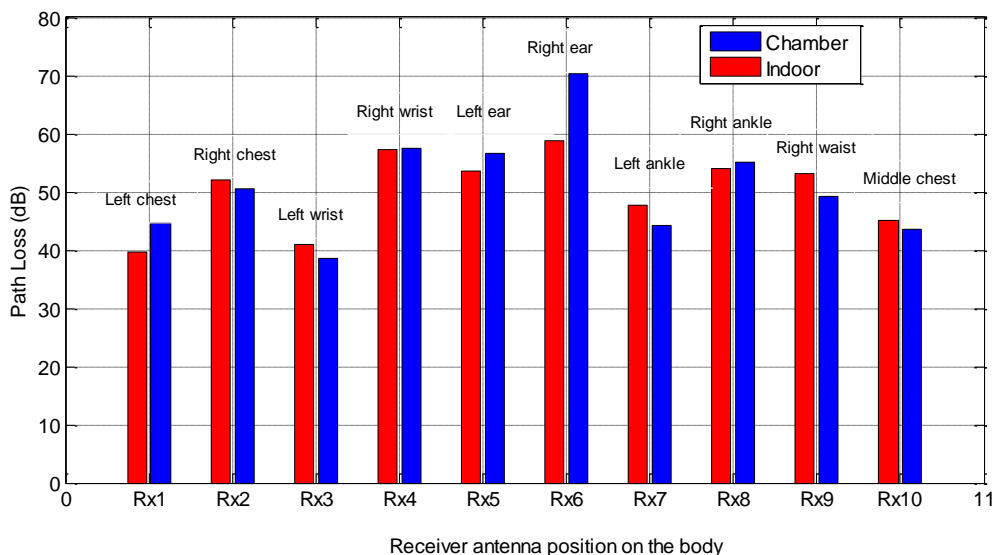


**Figure 12.** Comparison of path loss for left waist to 10 different on-body links at 2.45 GHz, measured in the chamber and in an indoor environment, of the dual band PIFA.

#### 4. Investigation of Off-Body Radio Propagation Channels at 1.9 GHz

##### 4.1. Path Loss vs. Distance

The path loss was modeled as a function of distance for 30 different receiver locations at 1.9 GHz in this section (Figure 13b). The off-body radio propagation performance of the dual band PIFA at 1.9 GHz was investigated. The off-body radio propagation channel measurement at 1.9 GHz is performed in the Body-Centric Wireless Sensor Laboratory at Queen Mary, University of London. A receiver dual band PIFA connected with Vector Network Analyzer (VNA) was placed on the ceiling near the wall, as shown in Figure 13b. The transmitter antenna connecting with the other port of the VNA was attached to five different locations on the human body, including right chest, left waist, left wrist, right ear, and left ankle, as shown in Figure 13a. During the measurement, the test subject was standing still at one to six meter locations with the interval of one meter facing towards the receiver antenna. For each transmitter antenna location and measurement scenario, ten sweeps were considered. The path loss for each different off-body channel is calculated directly from the measurement data S21 (10 sweep) averaging at 1.9 GHz.

A least square fit technique is performed on measured path loss for all five off-body channels (1~6 m) at 30 different transmitter locations to extract the path loss exponent (see Table 4). Figure 14 shows the measured value and modeled path loss for off-body channel vs. logarithmic transmitter (Tx)-Receiver (Rx) separation distance showing path loss exponent for the dual band PIFA at 1.9 GHz. The path loss exponent for off-body radio propagation at 1.9 GHz of the dual band PIFA is found to be



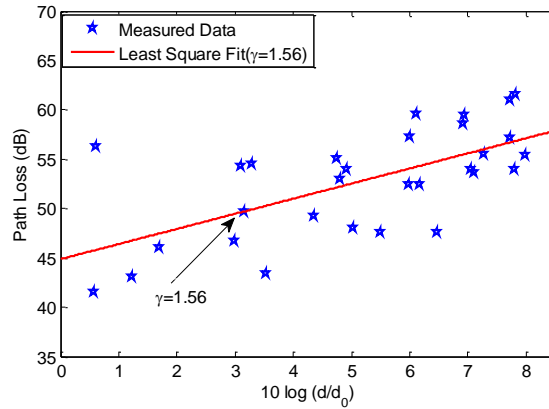


**Figure 14.** Measured and modeled path loss for off-body channel vs. logarithmic transmitter (Tx) and receiver (Rx) separation distance 1.9 GHz for the dual band PIFA.

**Table 4.** Off-body path loss parameters at 1.9 GHz.

Path Loss Parameters	Results
$\gamma$	1.56
$PL_{dB}(d_0)$ (dB)	44.9
$\sigma$ (dB)	4.12

Figure 15 shows the deviation of measurements from the average path loss fitted to a normal distribution for the dual band PIFA at 1.9 GHz for off-body propagation. In the indoor, the standard deviation of the normal distribution for this dual band PIFA is  $\sigma = 4.12$ .

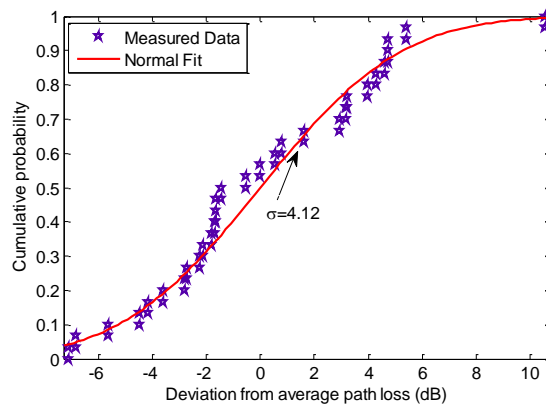


**Figure 15.** Deviation of measurement from the average path loss (fitted to normal distribution) of the dual band PIFA for off-body radio propagation channel at 1.9 GHz.

4.2. Off-Body Radio Channel Path Loss Characterization at 1.9 GHz

In this section, off-body radio propagation channel at 1.9 GHz of the dual band PIFA has been characterized. Five different off-body radio channels (right chest, left waist, left wrist, right ear and left ankle) were considered (Figure 13a). The measured path loss data for these five off-body radio channels were extracted from the previous measurement results of 1.9 GHz off-body measurement case. Figure 16 shows the comparison of path loss for five different off-body radio channels, when subject was standing still at one to six meter locations measured in the indoor environment. At one-meter distance location, the

lowest path loss value is noticed for the receiver to the chest link and the highest path loss value is noticed at the ear and ankle links. The chest link has the lowest communication distance and Line-of-Sight (LoS) communication with the receiver antenna as compared to the ankle link resulting the lowest path loss value for this link. Though, the communication distance between the receiver antenna and the right ear link is less but higher path loss value is noticed for this link, which is due to the different orientation of the transmitter antenna located on the right ear. For off-body radio propagation, the position of the antenna on the human body is also very important. At one meter distance, the average path loss of five off-body links is 47.37 dB, while at six meter distance, it is 57.84 dB. Results show that as the distance increases, the path loss for most of the off-body radio channels increases. This dual band PIFA shows good off-body radio propagation channel performance at 1.9 GHz.

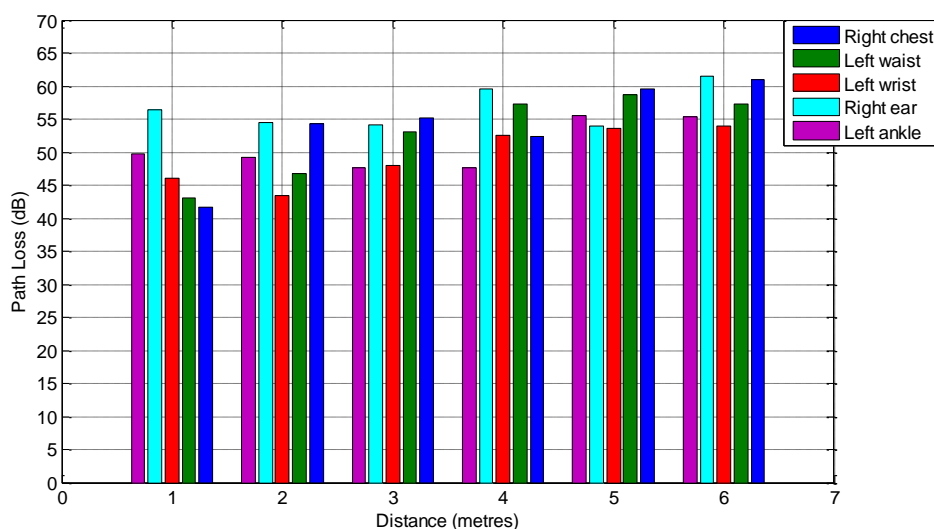


**Figure 16.** Comparison of path loss for five different off-body channels at 1.9 GHz measured using dual band PIFA, when subject was standing still at 1–6 m locations in sensor laboratory.

### 5. Conclusions

A dual band planar inverted F antenna (PIFA) is designed for cooperative on-body and off-body communications to be applied in healthcare applications. The performance parameters in close proximity of the proposed dual band PIFA have been investigated. Results and analysis show that the performance parameters of the proposed dual band PIFA are not affected much by the human body effects. The antenna shows very good on-body performance when placed very close to the human body. The on-body radio channel behavior at 2.45 GHz of this PIFA has been experimentally investigated in the anechoic chamber and in an indoor environment. In addition, the off-body radio channel behavior of this dual band PIFA at 1.9 GHz has been investigated in an indoor environment. The path loss exponent for on-body propagation at 2.45 GHz and off-body propagation at 1.9 GHz has been extracted and analyzed. In addition, the on and off-body radio channel characterization has been investigated and analyzed. The antenna has compact size and it shows very good on-body and off-body radio channel performance. Based on the results and analysis, this compact dual band PIFA will be very good candidate for on and off-body communications in healthcare applications.

## Acknowledgments

The authors of this paper would like to thank John Dupuy for his help with the antenna fabrication. The authors also would like to thank Sanjoy Mazumdar for his help during the measurement.

## Author Contributions

The research is mainly carried out by Mohammad Monirujjaman Khan. The paper is also written by Mohammad Monirujjaman Khan. Qammer H. Abbasi and Ratil Hasnat Ashique helped the main author (Mohammad Monirujjaman Khan) during measurement of the performance parameters of the antenna and also proofreading of the paper.

## Conflicts of Interest

The authors declare no conflict of interest.

## References

1. WSN for Healthcare: A Market Dynamics Report. Available online: <http://www.onworld.com/healthcare.index.html> (accessed on 7 August 2008).
2. Hall, P.S.; Hao, Y. *Antennas and Propagation for Body-Centric Wireless Communications*, 2nd ed.; Artech House: Norwood, MA, USA, 2006.
3. Alomainy, A.; Hao, Y.; Davenport, D.M. Parametric Study of Wearable Antennas Varying Distances from the Body and Different On-Body Positions. In Proceedings of the IET Seminar on Antennas and Propagation for Body-Centric Wireless Communications, London, UK, 24 April 2007; pp. 84–89.
4. Scanlon, W.G.; Evans, N.E. Numerical analysis of body worn UHF antenna systems. *Electron. Commun. Eng. J.* **2001**, *13*, 53–64.
5. Hall, P.S.; Hao, Y.; Nechayev, Y.I.; Alomainy, A.; Constantinou, C.C.; Parini, C.G.; Kamruddin, M.R.; Salim, T.Z.; Hee, D.T.M.; Dubrovka, R.; *et al.* Antennas and propagation for on body communication systems. *IEEE Antennas Propag. Mag.* **2007**, *49*, 41–58.
6. Alomainy, A.; Hao, Y.; Pasveer, F. Numerical and experimental evaluation of a compact sensor antenna for healthcare devices. *IEEE Trans. Med. Circuits Syst.* **2007**, doi:10.1109/TBCAS.2007.913127.
7. Conway, G.A.; Scanlon, W.G. Antennas for over body-surface communication at 2.45 GHz. *IEEE Trans. Antennas Propag.* **2009**, *57*, 844–855.
8. Scanlon, W.G.; Chandran, A. Stacked-patch antenna with switchable propagation mode for UHF body-centric communications. In Proceedings of the IEEE International Workshop on Antenna Technology (IWAT), Santa Monica, CA, USA, 2–7 March 2009.
9. Alomainy, A.; Hao, Y.; Owadally, A.; Parini, C.G.; Hall, P.S.; Constantinou, C.C. Statistical analysis and performance evaluation for on-body radio propagation with microstrip patch antennas. *IEEE Trans. Antenna Propag.* **2007**, *55*, 245–248.
10. Nechayev, Y.I.; Hall, P.S.; Hu, Z.H. Characterisation of narrowband communication channels on the human body at 2.45 GHz. *IET Microw. Antenna Propag.* **2010**, *4*, 722–732.

11. Cotton, S.L.; Scanlon, W.G. An experimental investigation into the influence of user state and environment on fading characteristics in wireless body area networks at 2.45 GHz. *IEEE Trans. Wirel. Commun.* **2009**, *8*, 6–12.
12. Hausman, S.; Januszkiewicz, L. Impact of indoor environment on path loss in body area networks, *Sensors* **2014**, *14*, 19551–19560.
13. Khan, M.M.; Abbasi, Q.H.; Alomainy, A.; Parini, C. Experimental investigation of subject-specific on-body radio propagation channels for body-centric wireless communications. *Electronics* **2014**, *3*, 26–42.
14. Khan, M.M.; Monsurul Alam, A.K.M.; Kumer, P. Investigation of a compact ultra wideband antenna for wearable applications. *Int. J. Commun. Antenna Propag.* **2014**, *4*, 124–129.
15. Khan, M.M.; Abbasi, Q.H.; Rahman, M.; Ashique, R.H. Experimental Study of On-Body Radio Channel Performance of a Compact Ultra Wideband Antenna. *J. Electromagn. Anal. Appl.* **2015**, *7*, 1–9.
16. Abbasi, Q.H.; Khan, M.M.; Alomainy, A.; Hao, Y. Radio Channel Characterisation and OFDM-Based Ultra Wideband System Modelling for Body-Centric Wireless Networks. In Proceedings of the International Conference on Body Sensor Networks (BSN'11), Dallas, TX, USA, 23–25 May 2011; pp. 89–94,
17. Sun, Y.Y.; Cheung, S.W.; Yuk, T.I. Planar monopoles with different radiator shapes for UWB Body-Centric Wireless Communications. *J. Eng.* **2013**, doi:10.1155/2013/683428.
18. Abbasi, Q.H.; Khan, M.M.; Liaqat, S.; Kamran, M.; Alomainy, A.; Hao, Y. Experimental investigation of ultrawide band diversity techniques for on-body radio communications. *Prog. Electromagn. Res. C* **2013**, *34*, 165–181.
19. Sani, A.; Hao, Y. Modeling of path loss for ultrawide band body centric wireless communications. In Proceedings of the International Conference on Electromagnetics in Advance Applications, Torino, Italy, 14–18 September 2009; pp. 998–1001.
20. Alabidi, E.S.; Kamarudin, M.R.; Rahman, T.A.; Khalily, M.; Abdulrahman, A.Y.; Jamlos, M.F.; Jais, M.I. Radiation characteristics improvement of monopole antenna for WBAN applications. *Int. J. Multimed. Ubiquitous Eng.* **2014**, *9*, 53–64.
21. Sagor, M.H.; Abbasi, Q.H.; Alomainy, A.; Hao, Y. Compact and conformal ultra wideband antenna for wearable applications. In Proceedings of the 5th European Conference on Antenna and Propagation, Rome, Italy, 11–15 April 2011.
22. Rahman, A.; Alomainy, A.; Hao, Y. Compact body-worn coplanar waveguide fed antenna for UWB body-centric wireless communications. In Proceedings of the European Conference on Antenna and Propagations (EuCAP), Edinburgh, UK, 11–16 November 2007.
23. Klemm, M.; Kovcs, I.Z.; Pedersen, G.F.; Troster, G. Novel small-size directional antenna for UWB WBAN/WPAN applications. *IEEE Trans. Antennas Propag.* **2005**, *53*, 3884–3896.
24. See, T.S.P.; Zhi-Ning, C. Experimental characterization of UWB antennas for on-body communications. *IEEE Trans. Antennas Propag.* **2009**, *57*, 866–874.
25. Khan, M.M.; Abbasi, Q.H.; Alomainy, A.; Hao, Y. Performance of ultra wideband wireless tags for on-body radio channel characterisation. *Int. J. Antennas Propag.* **2012**, *2012*, 1–10.



26. Khan, M.M.; Abbasi, Q.H.; Alomainy, A.; Hao, Y.; Parini, C. Experimental characterisation of ultra-wideband off-body radio channels considering antenna effects. *IET Microw. Antennas Propag.* **2013**, *7*, 370–380.
27. Khan, M.M.; Abbasi, Q.H.; Alomainy, A.; Hao, Y. Study of Line of Sight (LOS) and Non Line of Sight (NLOS) Ultrawideband Off-Body Radio Propagation for Body-centric Wireless Communications in Indoor. In Proceedings of the 5th European Conference on Antennas and Propagation (EUCAP, 11), Rome, Italy, 11–15 April 2011; pp. 110–114.
28. Balanis, C.A. *Antenna Theory Analysis and Design*, 3rd ed.; John Wiley and Sons, Inc.: Hoboken, NJ, USA, 2005.
29. Electronic imaging: Board of regents. National Institute of Health National Library of Medicine USA, Bard of regents, Bethesda, MD, Technical Report NH 90–2197, 1990. Available online: <http://www.brooks.af.mil/AFRL/HED/hedr> (accessed on 20 October 2010).
30. Gabriel, C.; Gabriel, S. Compilation of the dielectric properties of body tissues at RF and microwave frequencies, 1999. Available Online: <http://www.brooks.af.mil/AFRL/HED/hedr/reports/dielectric/Title/Title.html> (accessed on 5 November 2010).
31. Calculation of the dielectric properties of body tissues. Institute for Applied Physics, Italian National Research Council. Available online: <http://niremf.ifac.cnr.it/tissprop/> (accessed on 5 November 2010).
32. Alomainy, A.; Sani, A.; Rahman, A.; Santas, J.G.; Hao, Y. Transient characteristics of wearable antennas and radio propagation channels for ultra-wideband body-centric wireless communications. *IEEE Trans. Antennas Propag.* **2009**, *57*, 875–884.
33. Gassezadeh, S.S.; Jana, R.; Rice, C.W.; Turin, W.; Tarohk, V. A statistical path loss model for in-home UWB channels. In Proceedings of the IEEE Conference on Ultrawide Band Systems and Technologies, Baltimore, MD, USA, 21–23 May 2002; p. 5964.
34. Abbasi, Q.H.; Sani, A.; Alomainy, A.; Hao, Y. On-Body Radio Channel Characterisation and System-Level Modelling for Multiband OFDM Ultra Wideband Body-Centric Wireless Network. *IEEE Trans. Microw. Theory Tech.* **2010**, *58*, 3485–3492.

© 2015 by the authors; licensee MDPI, Basel, Switzerland. This article is an open access article distributed under the terms and conditions of the Creative Commons Attribution license (<http://creativecommons.org/licenses/by/4.0/>).